Virus Research 304 (2021) 198544

Contents lists available at ScienceDirect

Virus Research

journal homepage: www.elsevier.com/locate/virusres

Application of quantitative immunofluorescence assays to analyze the expression of cell contact proteins during Zika virus infections

Santiago Leiva [a,1], María Paula Dizanzo [a,1], Cintia Fabbri [b], Marina Bugnon Valdano [a], Victoria Luppo [b], Silvana Levis [b], Ana Laura Cavatorta [a], María Alejandra Morales [b], Daniela Gardiol [a,*]

[a] Instituto de Biología Molecular y Celular de Rosario-CONICET, Facultad de Ciencias Bioquímicas y Farmacéuticas, Universidad Nacional de Rosario, Suipacha 531, 2000 Rosario, Argentina

[b] Instituto Nacional de Enfermedades Virales Humanas "Dr. Julio Maiztegui" (INEVH-ANLIS), Monteagudo 2510, Pergamino, Buenos Aires, Argentina

ARTICLE INFO

Keywords:
ZIKV
Cell contacts
DLG1
Occludin
Quantitative immunofluorescence

ABSTRACT

Zika Virus (ZIKV) is an RNA virus that belongs to the Flavivirus (FV) genus. In the last years, several unique characteristics of ZIKV among FV have been revealed, as the multiple routes of transmission and its ability to reach different human tissues, including the central nervous system. Thus, one of the most intriguing features of ZIKV biology is its ability to cross diverse complex biological barriers. The main aim of this study is to contribute to the understanding of the still unclear mechanisms behind this viral activity. We investigated an African strain and two South American ZIKV isolates belonging to the Asian lineage, in order to characterize possible differences regarding their ability to disturb intercellular junctions. The Asian isolates correspond to an imported (Venezuelan) and an autochthonous (Argentinian) ZIKV strain for which there is still no data available. We focused on occludin and DLG1 expression as markers of tight and adherent junctions, respectively. For this, we applied a quantitative immunofluorescence assay that can ascertain alterations in the cell junction proteins expression in the infected cells. Our findings indicated that the different ZIKV strains were able to reduce the levels of both polarity proteins without altering their overall cell distribution. Moreover, the grade of this effect was strain-dependent, being the DLG1 reduction higher for the African and Asian Venezuelan isolates and, on the contrary, occludin down-regulation was more noticeable for the Argentinian strain. Interestingly, among both junction proteins the viral infection caused a relative larger reduction in DLG1 expression for all viruses, suggesting DLG1 may be of particular relevance for ZIKV infections. Taken together, this study contributes to the knowledge of the biological mechanisms involved in ZIKV cytopathogenesis, with a special focus on regional isolates.

1. Introduction

Zika Virus (ZIKV) is a member of the Flavivirus (FV) genus, bearing a positive RNA genome that encodes three structural (capsid [C], premembrane/membrane [prM/M], envelope [E]) and seven non-structural (NS) proteins. It was discovered in Africa in 1947 and its impact on Public Health seemed restricted to sporadic cases associated with mild fever or asymptomatic infections. In 2014 ZIKV was introduced into the Americas, where it surprisingly spread rapidly. Likewise, a large number of infections during the last outbreaks revealed a previously unrecognized link between infection in pregnant women and congenital diseases that affected neurological development of their babies (Hamel et al., 2016; Merfeld et al., 2017).

Phylogenetic analyses of different ZIKV isolates have revealed two major lineages, African and Asian, the latter of which includes the strains responsible for the recent epidemic bursts (Haddow et al., 2012;

Abbreviations: AJ, adherent junctions; BBB, blood-brain barrier; DLG1, human Disc Large 1; E, Envelope; FV, Flavivirus; hpi, hours post-infection; IF, Immunofluorescence; IJM, Image J Macro, MOI, multiplicity of infection; pfu, plaque-forming unit; RawIntDen, raw integrated density, ROI, regions of interest, TJ, tight junctions; ZIKV, Zika virus.

* Corresponding Author
E-mail address: dgardiol@yahoo.com.ar (D. Gardiol).

[1] Contributed equally to this work.

https://doi.org/10.1016/j.virusres.2021.198544
Received 25 June 2020; Received in revised form 10 May 2021; Accepted 4 August 2021
Available online 13 August 2021

Hamel et al., 2016; Lanciotti et al., 2016). A large number of cases occurred in Brazil in 2015, from where it has spread to Central and South America, Mexico and the Caribbean islands ("PAHO-Pan Am Health Org Zika virus 2016"). In Argentina, over the 2016–2018 period, ZIKV infections were detected in several provinces as well as ten microcephaly cases associated with ZIKV infection during pregnancy. From these microcephaly events, six were autochthonous and four were imported; all the cases presented microcephaly and facial skull disproportion; it was also observed ventriculomegaly and brain calcifications in seven and six cases, respectively (Tellechea et al., 2018, 2020). However, little is known about the replication capacity and the virulence of the different local viral isolates, either imported or autochthonous strains.

ZIKV is transmitted by mosquitoes of the genus *Aedes* and, unlike other FV, there is evidence for sexual and vertical transmission as well (Musso et al., 2015; Hamel et al., 2016; Miner et al., 2016; Musso & Gubler, 2016). Moreover, the presence of ZIKV was determined in different human fluids and tissues as semen, saliva, tears, urine, eyes, brain, testes, and female genital tract (Miner & Diamond, 2017; Paz Bailery et al., 2018). These features indicate that ZIKV can infect a variety of cells including a big number of epithelial ones. Hence, ZIKV constitutes an emerging virus able to cross different biological barriers using multiple infection routes. Consequently, the study of the pathways that this virus uses to achieve the infection and dissemination in the host is important to understand its complex biology.

Several studies have been aimed to elucidate the mechanisms behind ZIKV's capacity to specifically infect the fetus nervous system, due to the severity of the associated pathologies (Shao et al., 2016; Wen et al., 2017; Alimonti et al., 2018). In this sense, the blood-brain barrier (BBB) works as a physical and immune protector that prevents pathogens and harmful blood substances from entering into the brain. The endothelial cells of the BBB bear tight (TJ) and adherent (AJ) junctions that limit the paracellular space and establish the apico-basal polarity, which is crucial for cell physiology (Maiuolo et al., 2018). In the case of neurotropic arboviruses, after inoculation through a mosquito bite, the virus replicates in the adjacent tissues and next spreads to the lymph nodes, where a subsequent replication occurs causing a viraemia (Ludlow et al., 2016). This viraemia is followed by viral spread to the nerve tissue, where it replicates in neurons (Suen et al., 2014). For the success of this process, the virus must cross multiple layers of polarized cells, including the BBB (Turtle et al., 2012). In line with this, it was shown that neurotropic FV are capable to interfere with the intercellular junctions. Western Nile virus, Tick-borne encephalitis virus and Japanese encephalitis virus have been associated with altered expression and/or distribution of proteins involved in the maintenance of cell-to-cell junctions, such as zonula occludens-1 (ZO-1), Claudin and occludin proteins (Suen et al., 2014; Bustamante et al., 2019).

In particular, for ZIKV, different studies have been carried out using *in vitro* models representative of the biological barriers that the virus must cross to produce the infection, such as the placenta and the BBB. Chiu and collaborators have demonstrated that ZIKV reduces the levels of ZO-1 and occludin TJ proteins inducing their proteasomal degradation in placental cells, promoting changes in the permeability and eventually favoring the passage of the virus particles through the host barriers (Chiu et al., 2020). However, ZIKV could infect endothelial cells without disrupting the TJ protein expression, suggesting that the virus crosses this specific BBB by a transcytosis mechanism (Chiu et al., 2020). On the other hand, it was shown that Claudin and occludin TJ proteins were down-regulated in infected endothelial cells using *in vitro* an *in vivo* models, and this was concurrent with changes in BBB permeability (Leda et al., 2019). Therefore, most of the studies until now have focused on the involvement of TJ in the maintenance of the barrier stability and its possible disruption during ZIKV infection. However, the results are somehow controversial according to the applied experimental system and further investigations are required using other ZIKV strains and cell models.

Conversely, the relevance of AJ proteins in ZIKV infection was far less investigated. Among the AJ proteins it is important to highlight the human Disc Large 1 protein (DLG1), a member of the Scrib polarity complex. DLG1 is a scaffolding protein that coordinates the assembly of multiprotein complexes involved in the control of cell polarity, cell division, cell migration, and intracellular trafficking (Knoblich, 2008; Walch, 2013; Golub, Wee, Newman, Paterson, & Prehoda, 2017; Stephens et al., 2018). In epithelial cells, DLG1 co-localizes with E-cadherin at the AJ in association with the cytoskeleton, where it has both structural and signaling functions (Roberts et al., 2012; Stephens et al., 2018). We have previously shown that DLG1 is a target of E6 high risk Human papillomavirus and Tax Human T cell leukaemia virus type 1 viral oncoproteins. The expression of these viral proteins induces changes in the levels and cell distribution of DLG1 with potential consequences in viral pathogenesis (Bugnon Valdano et al., 2016; Marziali et al., 2017; Dizanzo et al., 2020). Moreover, DLG1 is also targeted by viral proteins derived from Influenza A virus, Rabies virus, Human immunodeficiency virus and Adenovirus (for a review see Javier & Rice, 2011), and this issue was shown to be relevant either for virus infection or for virulence. Therefore, DLG1 appears to be a crucial cellular marker that is altered during infection with viruses from different families; however, with diverse outcomes in relation to DLG1 expression.

In line with all the expressed above, we here analysed DLG1 (AJ) and occludin (TJ) protein expression in ZIKV infected epithelial cells. We investigated two locally isolated ZIKV strains from the Asian lineage to characterize possible differences in their ability to disturb intercellular junctions. We analyzed in this study an imported and an autochthonous ZIKV strain previously isolated in Argentina and for which there is still no data available. We developed an algorithm to quantitatively and accurately assess junction proteins abundance and the subcellular distribution in infected cells using immunofluorescence assays. We also included in the analysis an African strain for comparison with the regional Asian isolates. We found that all the studied ZIKV strains were able to reduce the levels of both analyzed polarity proteins without altering their overall cell distribution. Moreover, the grade of this effect was strain-dependent and was not related to the viral replication and infection capacity. The results from this study contribute to the knowledge of the biological mechanisms involved in ZIKV cytopathogenesis, with a special focus on regional isolates.

2. Material and methods

2.1. Cell cultures

A549 human lung epithelial cells (ATCC CCL-185) and Vero E6 cells (ATCC® TL-1460) were grown in Minimum Essential Medium (EMEM, Gibco) supplemented with 1% L-glutamine, 100 U/ml penicillin, 100 g/ml streptomycin and 10% fetal bovine serum (Internegocios S. A.). The cell culture was maintained at 37 °C, in a 5% CO_2 atmosphere. All cell lines were regularly tested for mycoplasma contamination.

2.2. ZIKV strains and infection procedure

For this study three ZIKV strains were selected. Two of them were isolated in Argentina at the National Institute of Human Viral Deseases, "Dr.Julio I. Maiztegui (INEVH-ANLIS) and correspond to the Asian lineage: ZIKV ARCB116141 strain that obtained from a patient with a febrile syndrome who travelled from Venezuela to Argentina in 2016 (GenBank accession no. MK637519, indicated in the paper as "Venezuelan Asian" isolate or imported isolate), and ZIKV ARCH125797 strain, that was isolated in 2017 from a febrile case from Chaco province, Argentina (GenBank accession no. MK637518, indicated as "Argentinian Asian" isolate or autochthonous isolate). The third viral strain, MR-766, is from the African lineage (GenBank accession no. AY632535). The viral stocks were prepared after four passages in Vero E6 cells (ATCC® TL-1460) and conserved at −80 °C before cell infections. Viruses were tittered by plaque assays using Vero cells

according to the procedures of the INEVH (Russell et al., 1967; Stock titers: 3.0×10^6 pfu/ml; 1.8×10^6 pfu/ml and 7.5×10^6 pfu/ml for ZIKV ARCB116141, ZIKV ARCH125797, and MR-766 strains, respectively). For *in vitro* infections, A549 epithelial cells (600,000 cells per well) were exposed to ZIKV at a viral multiplicity of infection (MOI) of 0.025 for 1 h at 37 °C for each specific strain (5.0 µl for ZIKV ARCB116141, 83.0 µl ZIKV ARCH125797and 2.0 µl for MR-766 strains). Then, the inoculum was removed and the cells were washed with PBS (phosphate-buffered saline). Afterwards, infected cells were cultured in low serum medium to avoid cell overgrowth (EMEM medium supplemented with 2% fetal bovine serum, 1% L-glutamine, 100 U/ml penicillin and 100 g/ml streptomycin) for virus production during different times (0, 24 and 48 h) as indicated.

2.3. Viral rna isolation and rt-qpcr analysis

Viral RNA was purified from 140 µl of cell culture supernatant, using the QIAmp Viral RNA kit (QIAgen) according to the manufacturer's protocol. RNA was eluted into 60 µL of elution buffer and RT-qPCRs were performed using 5 µL of RNA and the SuperScript™ III Platinum™ One-Step qRT-PCR Kit (Invitrogen) in a Applied Biosystems 7500 Fast Real Time PCR System (Applied Biosystems). The assays were performed using the set of primer/probe 1086–1162c/1107-FAMas previously described by Lanciotti and collaborators (Lanciotti et al., 2008). The thermocycling conditions were: initiation for 30 min at 50 °C, followed by 2 min at 95 °C and 45 cycles of 15 seg at 95 °C and 1 min at 60 °C (Lanciotti et al., 2008; Santiago et al., 2013).

An ANOVA test followed by Tukey's multi-comparison test ($p_{value}<0.01$) was performed. The statistical analyses of these results were performed using the R software (R Core Team, 2018).

2.4. Immunofluorescence (IF)

A549 cells were grown on glass coverslips until 80% of confluence and next infected with one of three different ZIKV strains using a MOI of 0.025. Uninfected cell cultures were used as controls. At 48 h post infection (hpi) the cells were fixed for 20 min at room temperature in a 4% paraformaldehyde–PBS solution and permeabilized with 0.1% Triton X-100–PBS solution for 5 min at room temperature. After washing twice with PBS, the coverslips were incubated overnight at 4 °C with the corresponding primary antibody mix. The primary antibodies used were: polyclonal anti-NS3 ZIKV (kindly provided by Molecular Virology Laboratory, Instituto Fundación Leloir, Argentina (Gebhard et al., 2016)), anti-Flavivirus E-glycoprotein (DM4/4/D6/5 clone, Abcam, Cambridge, UK), anti-DLG1 (H-60 clone, Santa Cruz Biotechnology, Santa Cruz, CA, USA) and/or anti-occludin (71–1500 clone, ThermoFisher Scientific, Rockford, IL, USA). Later, the samples were incubated one hour at 37 °C with the secondary antibodies: Cy3 conjugated anti-mouse IgG (Chemicon International, Temecula, CA, USA) and ALEXA 488 conjugated anti-rabbit IgG (ThermoFisher Scientific, Rockford, IL, USA). Additionally, those coverslips which were incubated with a mix of anti-NS3 and anti-E primary antibodies were counterstain with 4′, 6-diamidino-2-phenylindole (DAPI). Finally, the samples were mounted onto glass slides using "Slow Fade" reagent (Molecular Probes, Thermo Fisher Scientific, Rockford, IL, USA).

Fluorescence microscopy images were acquired with a Carl Zeiss LSM880 confocal microscope following the sequential acquisition mode (Carl Zeiss, Germany). A 63x NA 1.4 plan apochromat oil immersion objective and a 20X NA 0.8 plan apochromat objective were employed. A 16-bits color scale was set for all images being compared.

2.5. Quantitative analysis of infection rate by if assays

This image analysis was performed using FIJI v1.52 software (Schindelin et al., 2012). The standards tools "color threshold" and "analyze particles" were applied to subtract the background and count the total number of nucleus and the single infected cells per image. The intensity of fluorescence signal that was considered as background was calculated as the threshold intensity level in which the uninfected control images reach an average intensity value of 0. In order to automatically analyze the input fluorescence images with high reproducibility and precision, an in-house macro code was written in "Image J Macro" (IJM) language. The same values of thresholding were applied to all the images being compared. As input, at least 30 fluorescence images per coverslip were used in order to get a representative sampling of the actual state of the cell culture to be evaluated. A Kruskal-Wallis test followed by Dunn's comparisons ($p_{value}<0.01$) was performed. The statistical analyses of these results were performed using the R software (R Core Team, 2018).

2.6. Quantitative analysis of the level and subcellular localization of DLG1 and occludin in infected cells by if assays

The image analyses were performed with FIJI v1.52 software (Schindelin et al., 2012). The segmentation plugin "Trainable Weka Segmentation v3.2.34″, a classification tool based on machine learning (Arganda-Carreras et al., 2017), was applied to each image to create a template that would automatically find the labeled cellular proteins associated with the cell membrane by providing examples of membranes and cytoplasm fluorescence signal. Each segmented image was converted into a binary mask and multiplied by the corresponding original image to obtain the final "classified image". Therefore, these images conserved the original value of the pixels associated with the membrane fluorescence signal, while assigned a value of 0 to each pixel associated with the cytoplasm. In order to process automatically the input fluorescence images, an "in-house" macro IJM code was written. To assess the fluorescence intensity in individual cells, regions of interest (ROIs) were manually outlined along cell perimeters to include the full membrane width and thickness using the original images. The fluorescence signal associated with the viral E protein allowed to discriminate between infected and uninfected cells.

On each original and classified image, DLG1 or occludin fluorescence was quantified as the sum of pixel intensities, expressed as raw integrated density (RawIntDen) per ROI. Therefore, the RawIntDen and the area of each ROI for the total pixels (original image) and only for the membrane pixels (classified image) were measured, while the corresponding cytoplasm RawIntDen and area were calculated as the difference of the previous values (membrane values subtracted from the total). Finally, these results were expressed as RawIntDen/Area to each outlined cell to avoid the bias due to the different cell areas. A Kruskal-Wallis test followed Dunn's comparisons ($p_{value}<0.01$) was performed. The statistical analyses of these results were performed using the R software (R Core Team, 2018). For detailed information see Supplementary File 1.

3. Results

3.1. Different zikv strains show distinct infection and replication capacities

A wide spectrum of relevant differences has been previously reported among ZIKV strains. Even single mutations have been associated with important changes in strain characteristics (Yuan et al., 2017). Particularly, we were interested in analyzing South American viral isolates from different geographical regions (Argentine autochthonous and Venezuela imported strains, both from the Asian lineage) to evaluate potential differences in viral replication performance and in comparison with the African lineage. For this, we analyzed the replication and infection capacity of each viral strain described in MM section. This data would be relevant for later correlate viral replication with the ability to disturb intercellular junctions.

On one hand, we evaluated viral replication by RT-qPCR assays to

measure the viral RNA produced during *in vitro* infections. A549 epithelial cells, which are permissive to ZIKV infection (Himmelsbach & Eberhard, 2018), were infected at a MOI of 0.025 with each one of the three different ZIKV strains. The viral genome was assessed at 0, 24 and 48 hpi and the data was used to calculate the ratio of new virions produced for each ZIKV strain under the same controlled conditions. The African isolate showed a significant higher ratio of viral RNA production when compared with the Asian strains at each time-point. Furthermore, no significant differences between the Asian regional isolates were detected, despite their different geographical origin (Fig. 1.A).

Next, we performed a series of quantitative IF assays to determinate the infection capacity of the different ZIKV strains. Given that no differences were observed between the regional isolates regarding viral replication we performed this experiment using only one of them. A549 cells were infected with the African and the Venezuelan Asian strains at a MOI of 0.025. At 48 hpi, the cells were immunostained for the E and NS3 viral proteins to detect the infected cells (Fig. 1B). Several micrographs of the IF assays were captured and used as the input to automatically count the number of infected cells using an "in-house" IJM code. Subsequently, these data were used to calculate the percentage of infected cells with each strain under the same controlled conditions. The results showed that the African strain reached a significant higher proportion of infected cells than the Venezuelan Asian one (Fig. 1.B and 1. C).

These findings suggest that the African strain has a higher replication rate than the Asian isolates and, in addition, was also associated with higher infection degree in these experimental conditions.

3.2. ZIKV infections alter occludin expression in epithelial cells

As described above ZIKV widely spreads across their hosts and in order to access different tissues, the virus particles must pass through complex biological barriers (Mlakar et al., 2016). However, the data about the actual mechanisms behind this are still unclear. Most reports refer to the alterations in TJ protein expression with some contradictory results accordingly to the virus strain or the cell type used in the analysis (Leda et al., 2019; Chiu et al., 2020).

We wanted to contribute to shed light into this issue by analyzing local viral isolates, not investigated up till now, and using the epithelial A549 cell model. We chose occludin as a TJ marker and we applied an assay based on the quantitative analysis of IF images for accurately detect possible and even subtle changes in the cell protein expression. This algorithm, which is based on imaging segmentation and subsequent fluorescence for the quantification, is capable to specifically discriminate the signal associated with the membrane from that corresponding to the cytoplasm. This characteristic allows detecting not only alterations in the overall level of occludin, but also possible changes in its subcellular distribution. Moreover, this test allows evaluating changes in a large number of properly identified infected cells. For this, A549 cells were infected at a MOI of 0,025 with the three different available ZIKV strains (African, Argentinian Asian and Venezuelan Asian) in order to assess possible diverse effects on the cell contacts. At 48 hpi, the cells were immnostained for the E viral protein and occludin by IF (Fig. 2A). From the analyses of more than 100 E protein positive images we observed that every ZIKV strain infection was associated to a decrease in the overall level of occludin compared with the uninfected cell culture control (Fig. 2B). However, this reduction was higher for the cells infected with the Argentinian Asian strain, which registered a decrease of about a quarter for the occludin signal (regarding the uninfected condition). Meanwhile the infected cells with the Venezuelan Asian and the African strains showed a decrease of just about one tenth comparing with the uninfected condition (Fig 2.B). Interestingly, for both Asian strains the occludin expression analysis showed specific reductions in both membrane and cytoplasm subcellular compartments to a similar extent to the changes observed for the overall occludin signal. Hence, no significant difference in the membrane/cytoplasm signal ratio was detected for cells infected with both Asian strains (Fig 2.C), where, however, most of the occludin expression remained associated with cell membrane (Fig 2A and C). Nevertheless, for the African strain a decrease was observed in the occludin fraction associated with the cytoplasm, resulting in a significant increase in the membrane/cytoplasm signal ratio compared to the uninfected control (Fig. 2C).

Therefore, the data suggest that ZIKV infection induces a slight but significant decrease in the overall level of occludin and the magnitude of these changes seems to be strain-dependent. The subcellular distribution of the TJ protein was not altered in cells infected with both regional strains. Meanwhile, the raise in the membrane/cytoplasm occludin expression ratio observed in African ZIKV infected cells might be likely due to a decrease in the cytoplasmic pool rather than protein cell redistribution.

3.3. ZIKV infections alter DLG1 expression in epithelial cells

As expressed before little information is available about the effect of ZIKV infection over AJ. In this sense we evaluated the expression of one of the Scrib polarity complex members, DLG1, which has an important role in the maintenance of cell polarity and the integrity of the intercellular junctions, and is also a target of diverse virus, as expressed before (Javier & Rice, 2011). For this, we performed the quantitative analysis of IF images previously described for occludin expression. At 48 hpi A549 cells independently infected with the three available ZIKV strains were immunostained for E viral protein and DLG1 by IF (Fig. 3A). From the analysis of about 100 images, it can be observed that infected cells with any of the ZIKV strains showed a significant decrease in overall DLG1 abundance compared with the uninfected control. These reductions were higher for the African and the Venezuelan Asian strains, which presented a decrease of about one half of the DLG1 signal compared to the uninfected condition. Meanwhile, the Argentinian Asian strain showed a decrease of about a quarter of the DLG1 signal (Fig 3.B). In all cases, both the DLG1 membrane and cytoplasm fractions were reduced to a similar degree to the changes observed for their respective global DLG1 signal. Subsequent analysis confirmed that there was no significant variation in the membrane/cytoplasm fractions ratio among the infected cells with the different ZIKV strains compared with the uninfected control (Fig 3.C). Moreover, as can be observed, most of the DLG1 expression remained associated with the membrane (Fig 3.A and C).

Therefore, ZIKV infection may induce a decrease in the overall level of DLG1 but does not change its normal subcellular localization. Besides, although the effect was observed for any of the analyzed ZIKV strains, the magnitude of the reduction was strain-dependent and this may be due to particular features of each viral isolate.

4. Discussion

Although ZIKV activity has decreased markedly in the American region between 2018 and 2020, the risk of serious new outbreaks remains, as the virus continues to circulate and has even spread to new regions. Therefore, and considering recent epidemic bursts, ZIKV constitutes a potential risk for a large part of the world, including our country, where the vector is already present in large urban areas (Tellechea et al., 2018, 2020). These observations, strongly suggest the importance of understanding the mechanisms involved in viral pathogenesis.

In the last years several studies reported new insights about viral mechanisms associated to the unique characteristics of ZIKV among the FV, like the several routes of transmission, and its ability to reach different human tissues (Musso & Gubler, 2016). One of the most intriguing features of ZIKV biology is its ability to cross several biological barriers composed of different cell types. The direct disruption of intercellular junctions, transcytosis and modulation of cytokine-mediated cell permeability are some of the diverse mechanisms

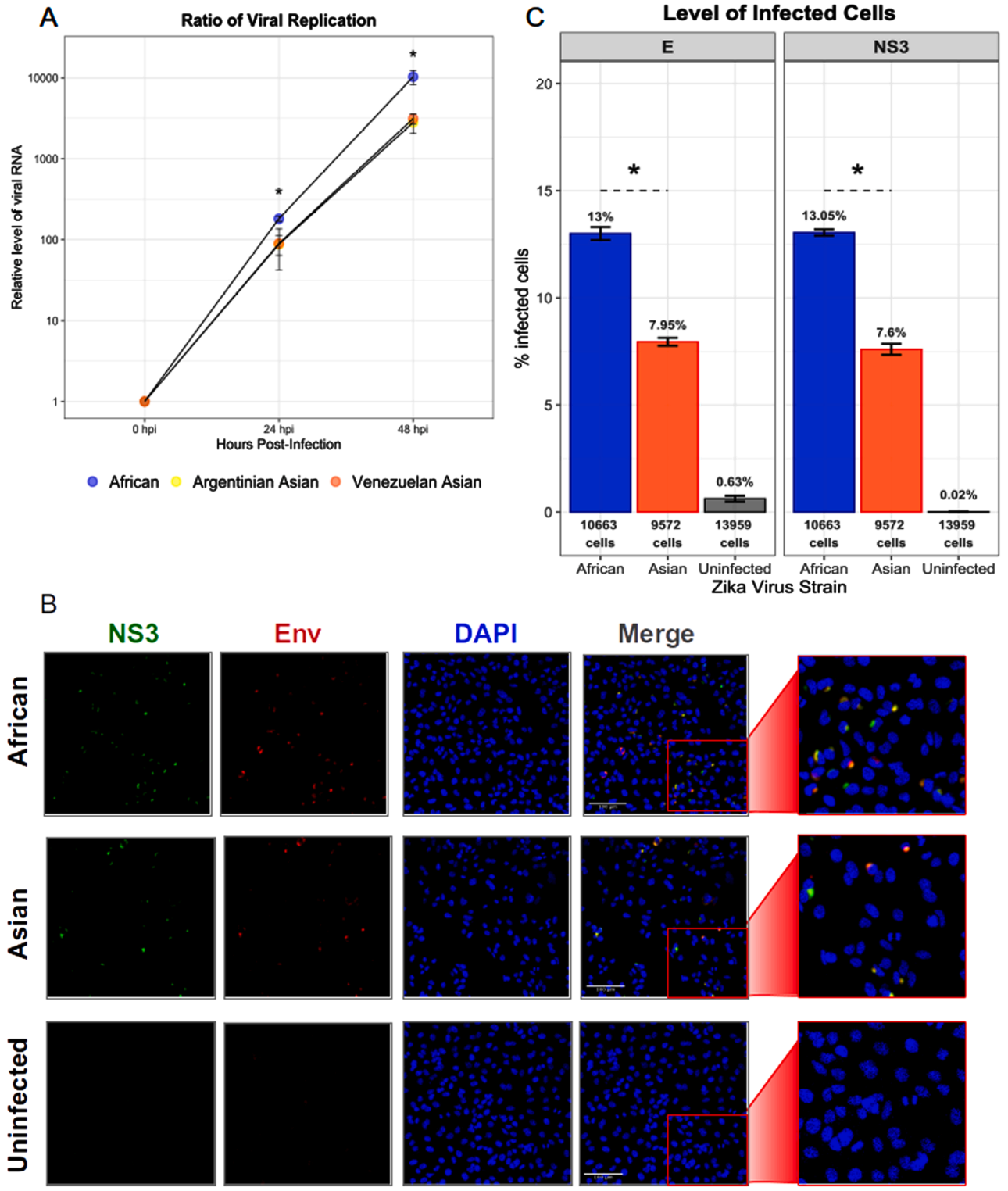

Fig. 1. Comparative analysis of infection and viral replication capacity of different ZIKV strains. A. A549 cells were infected with different ZIKV strains at a MOI of 0.025. The level of viral genome in the culture supernatant was assayed at different times post infection (0, 24 and 48 hpi) using RT-qPCR. The plot shows the relative increase of viral genome for each strain over time respect to the initial amount (0 hpi). The data represent 3 independent experiments. An ANOVA followed by Tukey's multi-comparison test ($p_{value}<0.01$) was performed. Asterisks denote significant difference between the African and the Asian strains for a particular condition. **B**. A549 cells were infected with different ZIKV strains at MOI: 0.025. At 48 hpi the cells were fixed and IF assays against the NS3 (green) and E (red) viral proteins were performed. The nucleus was counterstained with DAPI (blue). The bottom panels represent the uninfected condition. Representative images are shown. The images were acquired with a magnification of 20X. All scale bars represent 100 μm. **C.** The graphic shows the percentage of infected cells by the different viral strains (MOI: 0.025) at 48 hpi, as well as for uninfected cells, as an antibody control. The total number of counted cells for each condition is also indicated. A Kruskal-Wallis test followed by Dunn's comparisons ($p_{value}<0.01$) was performed. Asterisks denote significant difference among conditions. At least 30 fields were analyzed in each condition. These results represent 2 independent experiments.

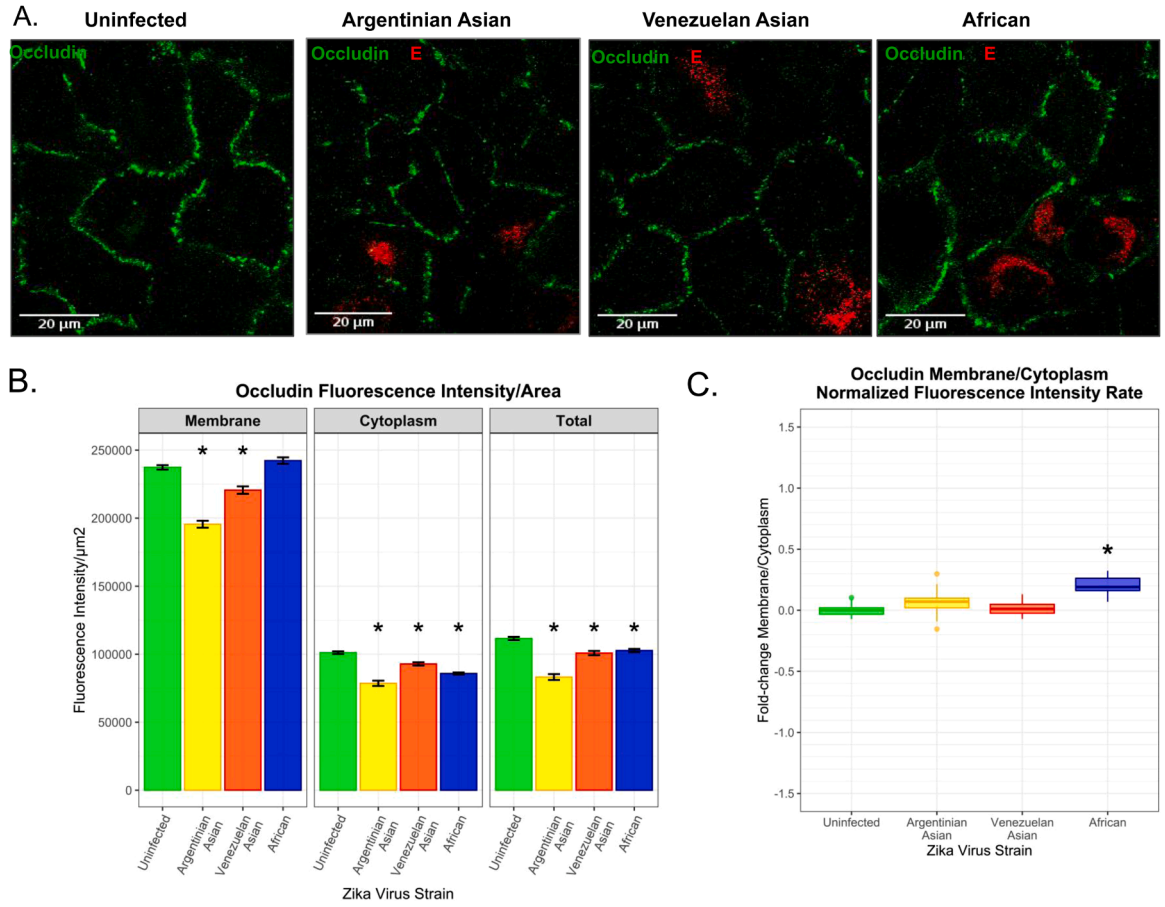

Fig 2. Quantitative analysis of the level and subcellular localization of occludin protein in ZIKV infected epithelial cells by IF assays. A. A549 cells were infected with different ZIKV strains at a MOI of 0.025. At 48 hpi the cells were fixed and the occludin cellular protein (green) and E the viral protein (red) were immunostained. Representative images are shown. The images were acquired with a magnification of 63X. All scale bars represent 20 µm. **B.** The Bar-plot shows the level of fluorescence signal associated to occludin protein expression per cell in different subcellular compartments. A Kruskal-Wallis test followed by Dunn's comparisons ($p_{value}<0.01$) was performed. 125 Z-projection using maximum intensity mode from 6 cell slides images were analyzed avoiding the bottom and top of the cell during the acquisition. Asterisks denote significant difference between a particular condition and the respective uninfected control. **C.** The box-plot shows the ratio between the DLG1 signal associated to the membrane and the cytoplasm per condition, normalized respect to the ratio value of the uninfected control. A Kruskal-Wallis test followed by Dunn's comparisons ($p_{value}<0.01$) was performed. Asterisks denote significant difference between a particular condition and the respective uninfected control.

that were described; however, with some controversial results (Papa et al., 2017; Leda et al., 2019; Chiu et al., 2020). We wanted to evaluate this issue in regional ZIKV strains associated to the last outbreak in the Americas, since no reports about interferences with cell-to-cell contacts for the local isolates are available. Both investigated regional strains were isolated in Argentina but derived from different geographical areas and in different times, one imported from Venezuela (2016) and the other, an autochthonous case from the Chaco Argentinian province (2017).

First we evaluated the virus replication and infection capacity of the both regional isolates in comparison with the African prototype strain. We performed *in vitro* infections using the same MOI for each strain. The results showed higher infection and replication rates for the African strain comparing with the Asian regional ones. This is in agreement with some reports that showed a better replication performance for the African lineage (Simonin et al., 2016; Rossi et al., 2018). No differences were observed between both regional strains, although their different geographical origin and collection date. These experiments also demonstrated that 48 hpi and a MOI of 0.025 are suitable conditions for reaching replication and infection rates able to be detected by IF assays. Moreover, at the same time, the cell morphology of infected cells was sufficiently preserved to evaluate intercellular junction expression as required for the subsequent experiments.

Then we investigated the direct effect of the studied viral strains on cell-to-cell contact proteins, a major contradictory issue in previous reports from different authors. For this, we applied a quantification test that can ascertain even minor alterations in cell protein expression in the specific infected cells, which are identified by IF. An additional advantage of this assay is that it consents to measure protein abundance in the different cell compartments and hence protein cell distribution.

Our findings indicated that the three evaluated viral isolates were able to reduce the levels of occludin and the DLG1 proteins as TJ and AJ marker, respectively. Strikingly the Venezuelan and African lineages behaved in the same way regarding the reduction rate of the overall level of each cell junction marker, suggesting that the effect depends on each particular strain more than a particular lineage. The fact that the African strains were not associated with microcephaly or with recent outbreaks does not imply that this lineage is less cytopathogenic. Moreover, in different *in vivo* experimental settings the African lineage resulted in higher mortality and viral loads in several tissues, thus is not surprising to find a similar behavior for both lineages (Simonin et al., 2017; Rossi et al., 2018). However, until now we cannot precisely correlate changes in cell contact protein expression and viral replication or pathogenesis and further studies are required to precisely understand the involvement of these cell proteins in virus behavior.

Regarding the integrity of TJ, occludin reduction was observed in

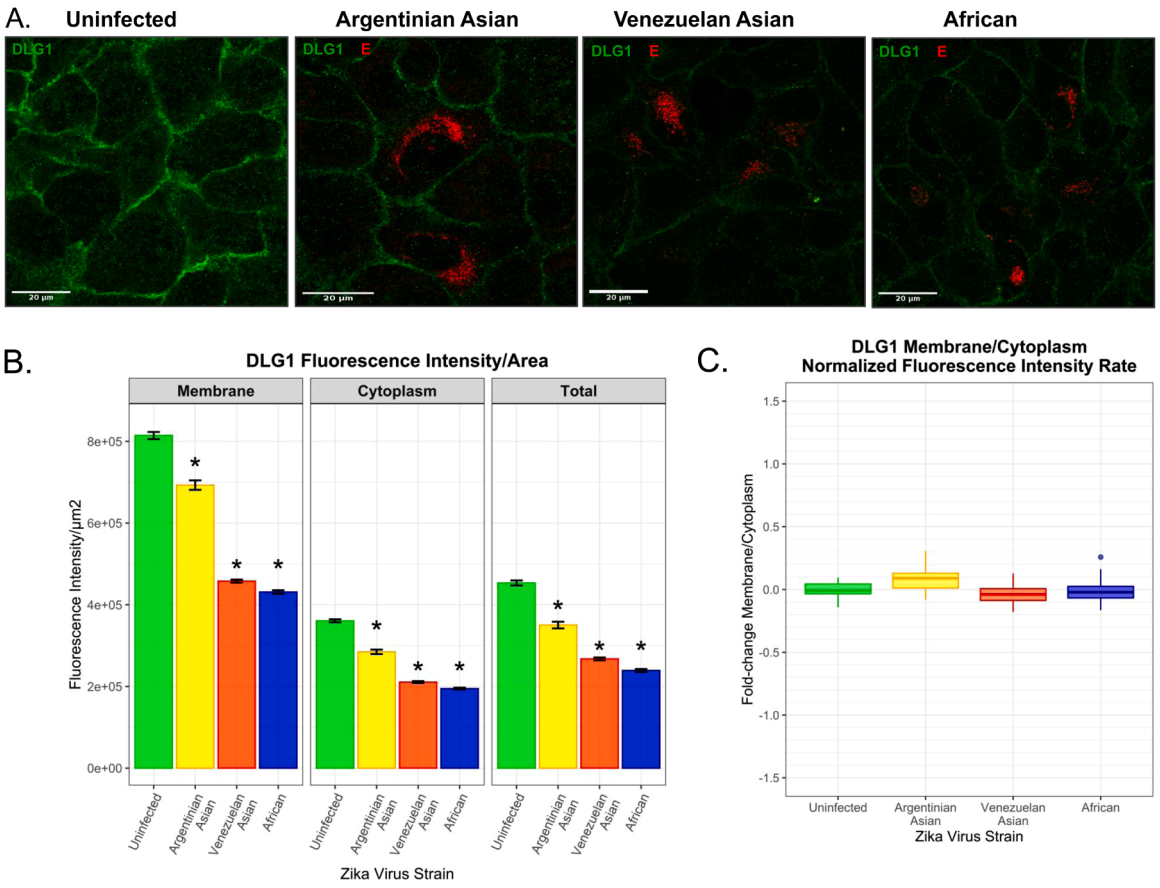

Fig 3. Quantitative analysis of the level and subcellular localization of DLG1 in ZIKV infected epithelial cells by IF assays. A. A549 cells were infected with different ZIKV stranis with a MOI of 0.025. At 48 hpi the cells were fixed and the DLG1 cellular protein (green) and the E viral protein (red) were immunostained. Representative images are shown. The images were acquired with a magnification of 63X. All scale bars represent 20 µm. **B**. The Bar-plot shows the level of fluorescence signal associated to DLG1 protein expression per cell in different sub-cellular compartments. 120 micro-photographs were analyzed. A Kruskal-Wallis test followed by Dunn's comparisons ($p_{value}<0.01$) was performed. Asterisks denote significant difference between a particular condition and the respective uninfected control. **C**. The box-plot shows the ratio between the DLG1 signal associated to the membrane and the cytoplasm per condition, normalized respect to the ratio value of the uninfected control. A Kruskal-Wallis test followed by Dunn's comparisons ($p_{value}<0.01$) was performed. No significant differences were detected.

endothelial cells by Leda and collaborators (Leda et al., 2019) while other authors reported occludin down-regulation in placental cells, in association with increased proteasome degradation (Chiu et al., 2020). In most cases, and in agreement with our results, the effect was shown to be highly viral isolate-dependent. However, it is still not clear which is the real impact of changes in cell contact protein expression over the ability of viral particles to cross host barriers to infect different tissues. Some authors have proposed that transcytosis as well as basolateral release from endothelial infected cells without losing endothelial integrity, may allow infectious virus particles to cross the monolayers (Papa et al., 2017). Moreover, recent reports have suggested that, even in the absence of ZIKV active replication, secreted ZIKV NS1 protein is in part responsible for the disruption of endothelium, increasing the permeability and modulating the virus dissemination (Puerta-Guardo et al., 2019). Therefore, more than one pathway may probably favor the virus spread depending on the infection conditions.

In line with the expressed above, our results showed that although the level of occludin and DLG1 are diminished in ZIKV infected cells, most of the residual protein maintains their proper cell localization in association to cell membrane at the cell-to-cell contacts. This last might be especially apparent for the occluding TJ protein in cells infected with the African strain, where it seems that the membrane-related fraction may remain unaltered. Hence, the integrity of the junctions may be still conserved to certain degree in these experimental conditions and, probably, giving some advantages to the virus life cycle. At this stage it is not so clear if the reduction in these cell markers is due directly to viral components or to an indirect mechanism induced by the virus, such as cytokines or other cellular factors that may be involved in the regulation of the junction protein expression.

Noticeable all viral isolates reduce DLG1 to a relative higher extent than for occludin, suggesting that altered pathways during ZIKV infection could particularly regulate this AJ protein. It is worth to mention that DLG1 is involved in many cellular processes that the virus subverts in the infected cells. For example it is well known that FV uses cellular trafficking and secretory pathways where DLG1 may play a regulatory role (Walch, 2013; Sager et al., 2018).

5. Conclusions

In summary we analyzed the infection/replication capacity of two South American ZIKV Asian isolates and their effect on cell junction protein expression in comparison with the African lineage. For this, we performed a fluorescence quantification assay that results in a proper tool to specifically evaluate changes in protein expression in the infected cells. We demonstrated that infections with the regional viral strains reduce both occludin TJ and DLG1 AJ protein level in a strain-dependent manner without significant changes in cell marker distribution. DLG1 misregulation was shown as an important trait in many human pathologies (Marziali et al., 2018) and to our knowledge this is the first report about the analysis of the differential expression of DLG1 during ZIKV infection. However, further investigations are required to understand the mechanisms and consequence of DLG1 reduction in the ZIKV

pathogenesis. This study contributes to the understanding of the association of ZIKV infection with intercellular contacts integrity.

Author statement

SL, MPD, CF and VL planned and performed experiments. SL, MPD and MBV, analysed data and wrote the paper. MAM, SL and ALC advised on the experiments and data analysis. DG designed the study, analysed data and wrote the paper.

Maria Paula Dizanzo and Santiago Leiva were supported by fellowships from CONICET and Agencia de Promoción Científica y Tecnológica, respectively. This work was supported by a research grant from the Agencia de Promoción Científica y Tecnológica (Argentina, PICT 2016–1725). Not role of funding.

Declaration of Competing Interest

The authors declare that they have no competing interests.

Acknowledgements

We gratefully acknowledge to Dolores Campos and Rodrigo Vena from Instituto de Biología Molecular y Celular de Rosario-CONICET for excellent technical support and help with cell culture and confocal laser microscopy and image software, respectively. We also want to thank to Dr Andrea Maiza and Dr Carmen Saavedra, from the Production Department of INEVH-ANLIS for continuous support with reagents and medium preparation. In addition, we acknowledge to the Molecular Virology Laboratory, Instituto Fundación Leloir, Argentina for kindly providing the anti-NS3 antibody. Dr. Valeria Sigot (Instituto de Investigación y Desarrollo en Bioingeniería y Bioinformática, Facultad de Ingeniería, Universidad Nacional de Entre Ríos, Oro Verde, Argentina) for helpful discussion about the immunofluorescence assays.

Supplementary materials

Supplementary material associated with this article can be found, in the online version, at doi:10.1016/j.virusres.2021.198544.

References

Alimonti, J.B., Ribecco-Lutkiewicz, M., Sodja, C., Jezierski, A., Stanimirovic, D.B., Liu, Q., Haqqani, A.S., Conlan, W., Bani-Yaghoub, M., 2018. Zika virus crosses an in vitro human blood brain barrier model. Fluids Barriers CNS 15, 1–9. https://doi.org/10.1186/s12987-018-0100-y.

Arganda-Carreras, I., Kaynig, V., Rueden, C., Eliceiri, K.W., Schindelin, J., Cardona, A., Seung, H.S., 2017. Trainable Weka Segmentation: A machine learning tool for microscopy pixel classification. Bioinformatics 33, 2424–2426. https://doi.org/10.1093/bioinformatics/btx180.

Bugnon Valdano, M., Cavatorta, A.L., Morale, M.G., Marziali, F., Lino, V.D.S., Steenbergen, R.D.M., Boccardo, E., Gardiol, D., 2016. Disc large 1 expression is altered by human papillomavirus E6 /E7 proteins in organotypic cultures of human keratinocytes 97, 453–462. https://doi.org/10.1099/jgv.0.000364.

Bustamante, F.A., Miró, M.P., Velasquéz, Z.D., Molina, L., Ehrenfeld, P., Rivera, F.J., Bátiz, F., 2019. Role of adherens junctions and apical-basal polarity of neural stem/progenitor cells in the pathogenesis of neurodevelopmental disorders: a novel perspective on congenital Zika syndrome. Transl Res 210, 1–23. https://doi.org/10.1016/j.trsl.2019.02.014.

Chiu, C.-F., Chu, L.-W., Liao, I.-C., Simanjuntak, Y., Lin, Y., Juan, C.-C., Ping, Y.-H., 2020. The Mechanism of the Zika Virus Crossing the Placental Barrier and the Blood-Brain Barrier. Front Microbiol 11, 1–15. https://doi.org/10.3389/fmicb.2020.00214.

Dizanzo, M.P., Marziali, F., Avalos, C.B., Valdano, M.B., Leiva, S., Cavatorta, A.L., Gardiol, D., 2020. HPV E6 and E7 oncoproteins cooperatively alter the expression of Disc Large 1 polarity protein in epithelial cells. Biol Chem 400, 699–719.

Gebhard, L.G., Iglesias, N.G., Byk, L.A., Filomatori, C.V, Maio, F.A.De, Gamarnik, A.V, 2016. A Proline-Rich N-Terminal Region of the Dengue Virus NS3 Is Crucial for Infectious Particle Production. J Virol 90, 5451–5461. https://doi.org/10.1128/JVI.00206-16.

Golub, O., Wee, B., Newman, R.A., Paterson, N.M., Prehoda, K.E., 2017. Activation of Discs large by aPKC aligns the mitotic spindle to the polarity axis during asymmetric cell division. Elife 6, e32137. https://doi.org/10.7554/eLife.32137.

Haddow, A.D., Schuh, A.J., Yasuda, C.Y., Kasper, M.R., Heang, V., Guzman, H., Tesh, R. B., Weaver, S.C., 2012. Genetic Characterization of Zika Virus Strains : Geographic Expansion of the Asian Lineage. PLoS Negl Trop Dis 6, e1477. https://doi.org/10.1371/journal.pntd.0001477.

Hamel, R., Li, F., Despr, P., Yssel, H., 2016. Zika virus: Epidemiology, clinical features and host-virus interactions. Microbes Infect 18, 441–449. https://doi.org/10.1016/j.micinf.2016.03.009.

Himmelsbach, K., Eberhard, H., 2018. Identification of various cell culture models for the study of Zika virus. World J Virol 7, 10–20. https://doi.org/10.5501/wjv.v7.i1.10.

Javier, R.T., Rice, A.P., 2011. Emerging theme: cellular PDZ proteins as common targets of pathogenic viruses. J. Virol. 85, 11544–11556. https://doi.org/10.1128/JVI.05410-11.

Knoblich, J.A., 2008. Mechanisms of Asymmetric Stem Cell Division. Cell 132, 583–597. https://doi.org/10.1016/j.cell.2008.02.007.

Lanciotti, R.S., Kosoy, O.L., Laven, J.J., Velez, J.O., Lambert, A.J., Johnson, A.J., Stan, S. M., Duffy, M.R., 2008. Genetic and Serologic Properties of Zika Virus Associated with an Epidemic, Yap State, Micronesia, 2007. Emerg. Infect. Dis. 14, 1232–1239. https://doi.org/10.3201/eid1408.080287.

Lanciotti, R.S., Lambert, A.J., Holodniy, M., Saavedra, S., Castillo, C., 2016. Phylogeny of Zika Virus in Western Hemisphere, 2015. Emerg Infect Dis 22, 933–935. https://doi.org/10.3201/eid2205.160065.

Leda, A.R., Bertrand, L., Andras, I.E., El-hage, N., Nair, M., Toborek, M., 2019. Selective Disruption of the Blood – Brain Barrier by Zika Virus. Front Microbiol 10, 1–14. https://doi.org/10.3389/fmicb.2019.02158.

Ludlow, M., Kortekaas, J., Herden, C., Hoffmann, B., Tappe, D., Trebst, C., Griffin, D., Brindle, H., Solomon, T., Brown, A., van Riel, D., Wolthers, K., Pajkrt, D., Wohlsein, P., Martina, B., Baumgärtner, W., Verjans, G., Osterhaus, A., 2016. Neurotropic virus infections as the cause of immediate and delayed neuropathology. Acta Neuropathol 131, 159–184. https://doi.org/10.1007/s00401-015-1511-3.

Maiuolo, J., Gliozzi, M., Musolino, V., Scicchitano, M., Carresi, C., Scarano, F., Bosco, F., Nucera, S., Ruga, S., Zito, M.C., Mollace, R., Palma, E., Fini, M., Muscoli, C., Mollace, V., 2018. The " Frail " Brain Blood Barrier in Neurodegenerative Diseases : Role of Early Disruption of Endothelial Cell-to-Cell Connections. Int J Mol Sci 19, 2693. https://doi.org/10.3390/ijms19092693.

Marziali, F., Bugnon Valdano, M., Brunet Avalos, C., Moriena, L., Cavatorta, A.L., Gardiol, D., 2017. Interference of HTLV-1 Tax Protein with Cell Polarity Regulators: Defining the Subcellular Localization of the Tax-DLG1 Interaction. Viruses 9, 355. https://doi.org/10.3390/v9120355.

Marziali, F., Dizanzo, M.P., Cavatorta, A.L., Gardiol, D., 2018. Differential expression of DLG1 as a common trait in different human diseases: an encouraging issue in molecular pathology. Biol. Chem. https://doi.org/10.1515/hsz-2018-0350.

Merfeld, E., Ben-avi, L., Kennon, M., Cerveny, K.L., 2017. Potential mechanisms of Zika-linked microcephaly. WIREs Dev Biol e273, 1–14. https://doi.org/10.1002/wdev.273.

Miner, J.J., Cao, B., Govero, J., Smith, A.M., Fernandez, E., Cabrera, O.H., Garber, C., Noll, M., Klein, R.S., Noguchi, K.K., Mysorekar, I.U., 2016. Zika Virus Infection during Pregnancy in Mice Causes Placental Damage and Fetal Demise Article. Cell 165, 1081–1091. https://doi.org/10.1016/j.cell.2016.05.008.

Miner, J.J., Diamond, M.S., 2017. Zika virus pathogenesis and tissue tropism. Cell Host Microbe 21, 134–142. https://doi.org/10.1016/j.chom.2017.01.004.

Mlakar, J., Korva, M., Tul, N., Popović, M., Poljšak-Prijatelj, M., Mraz, J., Kolenc, M., Resman Rus, K., Vesnaver Vipotnik, T., Fabjan Vodušek, V., Vizjak, A., Pižem, J., Petrovec, M., Avšič Županc, T., 2016. Zika Virus Associated with Microcephaly. N Engl J Med 374, 951–958. https://doi.org/10.1056/NEJMoa1600651.

Musso, D., Gubler, D.J., 2016. Zika Virus. Clin. Microbiol. Rev 29, 487–524. https://doi.org/10.1128/CMR.00072-15. Address.

Musso, D., Roche, C., Nhan, T., Robin, E., Teissier, A., Cao-lormeau, V., 2015. Detection of Zika virus in saliva. J. Clin. Virol. 68, 53–55. https://doi.org/10.1016/j.jcv.2015.04.021.

PAHO-Pan Am Health Org Zika virus 2016. [WWW Document], n.d. URL http://www.paho.org/hq/index.php?option=com_content&view=article&id=11585&Itemid=41688&lang=.

Papa, M., Meuren, L., Coelho, S., Lucas, Cg., Mustafá, Y., Lemos Matassoli, F., Silveira, P., Frost, P., Pezzuto, P., Ribeiro, M., Tanuri, A., Nogueira, M., Campanati, L., Bozza, M., Paula Neto, H., Pimentel-Coelho, P., Figueiredo, C., Aguiar, R., Arruda, L., 2017. Zika Virus Infects, Activates, and Crosses Brain Microvascular Endothelial Cells, without Barrier Disruption. Front. Microbiol. 8 https://doi.org/10.3389/fmicb.2017.02557.

Paz Bailery, G., Rosenberg, E.S., Doyle, K., MunozJordan, J., Santiago, G.A., Klein, L., Perez-Padilla, J., Medina, F.A., Waterman, S.H., Gubern, C.G., Alvarado, L.I., Sharp, T.M., 2018. Persistence of Zika Virus in Body Fluids - Final Report. N Engl J Med 379, 1234–1243. https://doi.org/10.1056/NEJMoa1613108.Persistence.

Puerta-Guardo, H., Glasner, D.R., Espinosa, D.A., Biering, S.B., Ratnasiri, K., Wang, C., Beatty, P.R., Harris, E., 2019. Flavivirus NS1 Triggers Tissue-Specific Vascular Endothelial Dysfunction Reflecting Disease Tropism. Cell Rep 26, 1598–1613. https://doi.org/10.1016/j.celrep.2019.01.036.

Roberts, S., Delury, C., Marsh, E., 2012. The PDZ protein discs-large (DLG): the ' Jekyll and Hyde ' of the epithelial polarity proteins. J Febs 279, 3549–3558. https://doi.org/10.1111/j.1742-4658.2012.08729.x.

Rossi, S.L., Ebel, G.D., Shan, C., Shi, P.-Y., Vasilakis, N., 2018. Did Zika Virus Mutate To Cause Severe Outbreaks? Trends Microbiol 26, 877–885. https://doi.org/10.1016/j.tim.2018.05.007.Did.

Russell, P., Nisalak, A., Sukhavachana, P., Vivona, S., 1967. A plaque reduction test for dengue virus neutralizing antibodies. J Immunol 99, 285–290.

Sager, G., Gabaglio, S., Sztul, E., Belov, G.A., 2018. Role of Host Cell Secretory Machinery in Zika Virus Life Cycle. Viruses 10. https://doi.org/10.3390/v10100559.

Santiago, G.A., Vergne, E., Quiles, Y., Cosme, J., Vazquez, J., Medina, J.F., Margolis, H., Mun, J.L., 2013. Analytical and Clinical Performance of the CDC Real Time RT-PCR Assay for Detection and Typing of Dengue Virus. PLoS Negl Trop Dis 7, e2311. https://doi.org/10.1371/journal.pntd.0002311.

Schindelin, J., Arganda-Carreras, I., Frise, E., Kaynig, V., Longair, M., Pietzsch, T., Preibisch, S., Rueden, C., Saalfeld, S., Schmid, B., Tinevez, J.Y., White, D.J., Hartenstein, V., Eliceiri, K., Tomancak, P., Cardona, A., 2012. Fiji: an open-source platform for biological-image analysis. Nat Methods 9, 676–682. . https://doi.org/nmeth.2019 [pii] 10.1038/nmeth.2019.

Shao, Q., Herrlinger, S., Yang, S., Lai, F., Moore, J.M., Brindley, M.A., Chen, J.-F., 2016. Zika virus infection disrupts neurovascular development and results in postnatal microcephaly with brain damage. Development 143, 4127–4136. https://doi.org/10.1242/dev.143768.

Simonin, Y., Loustalot, F., Desmetz, C., Foulongne, V., Constant, O., Fournier-wirth, C., Leon, F., Molès, J., Goubaud, A., Lemaitre, J., Maquart, M., Leparc-goffart, I., Briant, L., Nagot, N., Perre, P., Van De, Salinas, S., 2016. Zika Virus Strains Potentially Display Different Infectious Pro fi les in Human Neural Cells. EBioMedicine 12, 161–169. https://doi.org/10.1016/j.ebiom.2016.09.020.

Simonin, Y., Riel, D.Van, Perre, P.Van De, Rockx, B., Salinas, S., 2017. Differential virulence between Asian and African lineages of Zika virus. PLoS Negl Trop Dis 11, e0005821. https://doi.org/10.1371/journal.pntd.0005821.

Stephens, R., Lim, K., Portela, M., Kvansakul, M., Humbert, P.O., Richardson, H.E., 2018. The Scribble Cell Polarity Module in the Regulation of Cell Signaling in Tissue Development and Tumorigenesis. J. Mol. Biol 430, 3585–3612. https://doi.org/10.1016/j.jmb.2018.01.011.

Suen, W.W., Prow, N.A., Hall, R.A., Bielefeldt-ohmann, H., 2014. Mechanism of West Nile Virus Neuroinvasion: A Critical Appraisal. Viruses 6, 2796–2825. https://doi.org/10.3390/v6072796.

Team, R.C., 2018. R: A Programming Environment for Data Analysis and Graphics. R Foundation for Statistical Computing, Vienna, Austria.

Tellechea, A.L., Bidondo, M.P., Luppo, V., Baricalla, A., Liascovich, R., Fabbri, C., Morales, M.A., Groisman, B., Silva, M., Masi, P., Israilev, A., Rocha, M.R., Quaglia, M., Escalante, B., Villarreal, A., Antinori, M., Barbero, P., 2020. ZIKA VIRUS EMBRYOPATHY IN ARGENTINA : CLINICAL CHARACTERISTICS AND DIAGNOSIS IN NEWBORNS. Rev Fac Cien Med Univ Nac Cordoba 77, 100–105. https://doi.org/10.31053/1853.0605.v77.n2.26754.

Tellechea, A.L., Luppo, V., Morales, M.A., Groisman, B., Baricalla, A., Fabbri, C., Sinchi, A., Alonso, A., Gonzalez, C., Ledesma, B., Masi, P., Silva, M., Israilev, A., Rocha, M., Quaglia, M., Bidono, M.P., Liascovich, R., Barbero, P., 2018. Surveillance of microcephaly and selected brain anomalies in Argentina : Relationship with Zika virus and other congenital infections. Birth Defects Res 110, 1016–1026. https://doi.org/10.1002/bdr2.1347.

Turtle, L., Griffiths, M.J., Solomon, T., 2012. Review Encephalitis caused by flaviviruses. Q J Med 105, 219–223. https://doi.org/10.1093/qjmed/hcs013.

Walch, L., 2013. Emerging role of the scaffolding protein Dlg1 in vesicle trafficking. Traffic 14, 964–973. https://doi.org/10.1111/tra.12089.

Wen, Z., Song, H., Ming, G., 2017. How does Zika virus cause microcephaly ? Genes Dev 31, 849–861. https://doi.org/10.1101/gad.298216.117.

Yuan, L., Huang, X., Liu, Z., Zhang, F., Zhu, X., Yu, J., Ji, X., Xu, Y., Li, G., Li, C., Wang, H., Deng, Y., Wu, M., Cheng, M., Ye, Q., Xie, D., Li, X., Wang, X., Shi, W., Hu, B., Shi, P., Xu, Z., Qin, C.-F., 2017. A single mutation in the prM protein of Zika virus contributes to fetal microcephaly. Science (80-.) 358, 933–936. https://doi.org/10.1126/science.aam7120.